Multi-Lifting-Device UAV Autonomous Flight at Any Transition Percentage

C. De Wagter & D. Dokter & G. de Croon & B. Remes

Abstract Hybrid UAVs with hovering as well as fast forward flight capability or enhanced maneuverability are expected to become increasingly important. To approach the complex problem of autonomous flight in the full flight envelope of these transitioning or reconfiguring vehicles, a simple but powerful approach is presented. A traditional rotorcraft control strategy consisting of an attitude innerloop and position outerloop is enhanced with a lift allocation controller in between. By running several sub-controllers per lift-device, simplicity is kept while allowing sustained flight at any transitioning percentage for any number of lifting devices. The applications of this approach range from hover of fixedwings, or allowing easier fast forward flight of conventional rotorcraft to autonomous flight of most types of hybrid or reconfiguring UAVs. Flight test results are presented using the ATMOS hybrid UAV.

Christophe De Wagter

Micro Aerial Vehicle Lab, Faculty of Aerospace Engineering, Delft University of Technology, Kluyverweg 1, 2629HS Delft, the Netherlands, e-mail: C.deWagter@tudelft.nl

Dirk Dokter

Micro Aerial Vehicle Lab, Faculty of Aerospace Engineering, Delft University of Technology, Kluyverweg 1, 2629HS Delft, the Netherlands e-mail: D.Dokter@student.tudelft.nl

Guido de Croon

Micro Aerial Vehicle Lab, Faculty of Aerospace Engineering, Delft University of Technology, Kluyverweg 1, 2629HS Delft, the Netherlands e-mail: G.C.H.E.deCroon@tudelft.nl

Bart Remes

Micro Aerial Vehicle Lab, Faculty of Aerospace Engineering, Delft University of Technology, Kluyverweg 1, 2629HS Delft, the Netherlands e-mail: B.D.W.Remes@tudelft.nl

List of abbreviations

Abbreviation	Description
AHRS	Attitude and Heading Reference System
UAV	Unmanned Aerial Vehicle
LTP	Local Tangent Plane
NED	North East Down
RC	Remote Control
A/C	Aircraft
LD	Lift Device

List of symbols

Symbol	Description
$\mathbf{x}, \mathbf{y}, \mathbf{z}_{LTP}$	Position command in Local Tangent Plane NED frame.
$\ddot{\mathbf{x}}, \ddot{\mathbf{y}}, \ddot{\mathbf{z}}_{LTP}$	Acceleration commands in Local Tangent Plane NED frame.
$\ddot{\mathbf{x}}, \ddot{\mathbf{y}}, \ddot{\mathbf{z}}$	Acceleration commands.
$\mathbf{q}$	Attitude quaternion.
$\mathbf{q}_{RC}$	Attitude quaternion setpoint from remote input.
$\ddot{\mathbf{q}}$	Second derivative of attitude quaternion.
ϕ, θ, ψ	Attitude of the body in LTP NED, unless otherwise specified.
X, Y, Z_{body}	X/Y/Z-axis of the A/C.
$\varepsilon_{\%}$	Transition percentage.
cmd_{θ}	Desired roll angle.
$\mathbf{g}$	Earth's gravitational acceleration.
$f_{fixed-wing}$	Lift allocation controller in 100% fixed-wing mode.
cmd_{Thrust}	Thrust command.
$T_{nominal}$	Nominal desired cruise throttle.
$v_{climb_{set}}$	Desired climb speed.
$K_{V_z \Rightarrow T}$	Lift allocation fixed-wing throttle increment gain.
$K_{\ddot{x} \Rightarrow T}$	Lift allocation fixed-wing forward acceleration gain.
$K_{V_z \Rightarrow \theta}$	Lift allocation fixed-wing pitch pre climb gain.
$\mathscr{F}_{Lift}$	Lift coordinate system.
$\mathscr{F}_{Body}$	Body coordinate system.
$\mathscr{F}_{Lift_i}$	Lift device coordinate system of LD i.

1 Introduction

The majority of fully autonomous Unmanned Air Vehicles (UAVs) are either fixed-wing vehicles or hovering vehicles. This is remarkable as the concept of hybrid and transitioning vehicles has been around for several decades and advantages can be

numerous. More obvious examples of such advantages are the boost in range and endurance while maintaining vertical take-off and landing capability–in the case of a rotorcraft with a wing [2]. But more out-of-the-box concepts like the 3-pair of perpendicular rotor hexacopter [7] create a platform that can hover at any attitude. An X-configuration fixed wing can create much faster sideward accelerations boosting its maneuverability compared to conventional fixedwings. But it also allows for instance the pointing of a camera left and right without the need for a pan-tilt device. While most of these concepts face major problems in the case of a manned airframe, in the case of UAV many problems are not applicable. This sheds new light on several of the concepts and forms the basis for this research.

A lot of research is working on enlarging the usable MAV flight envelope of conventional concepts through control theory [18, 4, 17], or creating vehicles with exceptionally large flight envelopes without the need for complex control [6]. To enhance capabilities other projects tend to focus on adding more vehicles [20, 19] or more sensors [13, 3, 16, 22] without any change to the flight concept. For fixedwings, several projects have enlarged the flight envelope from fast forward flight up to hover [10, 12, 11, 9, 8]. However, only [8] reported continuous flight in between flight regimes. Finally a lot of studies gave separate attention to the transitioning aspects of hybrid UAV [14, 23, 15, 21].

This work proposes a more unified approach to hybrid UAVs with an unlimited amount of *lifting-devices*. The term *lifting-device* is used to refer to any wing , rotor or thruster that is capable of carrying the weight of the vehicle while sufficient moment generating actuators remain to fully control the vehicles attitude when that lift device is active. A control architecture is defined that allows sustained flight at any regime of every lifting device *and* in between, if the aerodynamics and control surfaces physically allow this.

Most of the research is performed on a UAV named *ATMOV*, which stands for Autonomous Transition Multi-rotor Observation Vehicle (Fig 1). As shown in Fig. 3, ATMOV is a wing with 4 rotors placed perpendicularly to the wing's lifting surface. Nevertheless, the theory and concepts are specially developed to be applicable to a wide variety of other concepts including all aforementioned configurations, and thus ranging from simple rotorcraft to fixedwings and even from hybrid to reconfiguring configurations such as tilting wings.

Section 2 explains the control strategy, followed by more details on the lift allocation in Sect. 3. The transition is explained in Sect. 4 while Sect. 5 elaborates on the guidance aspects of transition. Section 6 describes some extra problems that differ from conventional fixedwing and rotorcraft control before Sect. 7 show results of experiments.

2 Control Strategy

A common control architecture for hovering vehicles consists of an outerloop controlling the position and an innerloop for attitude [13, 4, 5, 11]. This approach is

Fig. 1 ATMOV: Autonomous
transition Multi-rotor Obser-
vation Vehicle. The ATMOV
has two sets of differently
sized counter rotating pro-
pellers with large folding
hover props for slow and
hovering flight and smaller
high pitch tip props for effi-
cient cruise. The hover yaw
control is performed with
aerodynamic actuators only
as the differently sized rotors
do not allow uncoupled yaw
generation without pitch or
roll.

augmented by defining a *lift allocation* block in between the inner- and outerloops
as illustrated in Fig. 2.

Fig. 2 Flightplan Loop, Po-
sition Control Loop and At-
titude Control Loop setup.
The inner and outer loops are
built up in a similar fashion.
Position and attitude setpoints
enter, a reference model tracks
the setpoints with the desired
dynamics, and the controllers
output acceleration and an-
gular acceleration commands
to match this desired dynam-
ics. For the outerloop this
acceleration command is now
mapped to one of the lifting
devices.
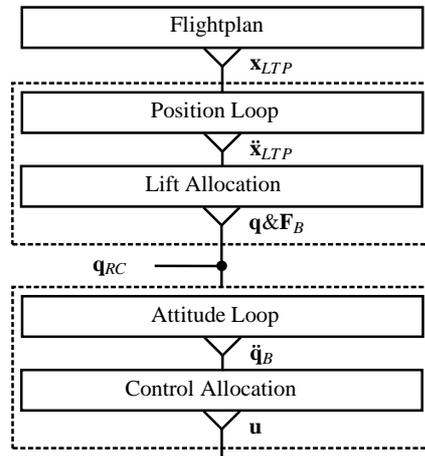
First the flight planning outputs a desired position **x** and desired attitude q in
function of time and position. Flightplan logic for instance activates the next part
of the flight plan when a waypoint is cleared. In forward flight the current desired
position—also called *carrot*—constantly moves in time [5].

The position command in local tangent plane x_{LTP} then enters the outerloop. A
non-linear reference model is selected to impose a desired closed loop response and
also impose rate limits. Any step changes now appear as continuous signals to the
linear PID compensator which generates acceleration commands $\ddot{\mathbf{x}}$. In conventional
rotorcraft control this desired acceleration is directly or implicitly mapped to an
attitude angle (Eq. 1), often applying a linearized thrust-vectoring model $\ddot{\mathbf{x}}_{cmd} \approx
g * cmd_\theta$.

This outerloop commanding accelerations and innerloop to control attitude can be applied to any type of vehicle. The only differences in control loops is in the way accelerations are mapped to attitude and thrusters. Two types of lift devices are defined at this point and referred to as wings and rotors. Now the lift allocation logic determines the active lifting devices and runs all the active sub-controllers, and combines the results into collective thrust and attitude. The attitude command continues to the inner loops, while direct thruster commands skip directly to the control allocation and supervision logic.

The innerloop takes a full attitude command as input. A second reference model removes unfeasible dynamics from the command, followed by a controller. Finally the control allocation with actuator supervision distributes the un-scaled actuator torque commands from the innerloop and the direct force commands from the outerloop to the corresponding actuators and rotors.

On ATMOV-like vehicles the pitching in hover is generated by increasing the nose rotor (direction of X_{body}) and reducing the $-X$ rotor, as well as deflecting both ailevons—which are combined aileron and elevators—in the $-X$ direction (Fig 3). The more the airspeed in the body $-Z$ direction (which is the direction of the wing), the smaller the needed deflections for a certain torque and the less rotors are effective. Gain scheduling is applied based on airspeed or transition percentage $\varepsilon_\%$.

3 Lift-Device Control Allocation

Similarly to the control allocation after the innerloop, the same idea is applied to the outerloop where lifting devices take the role of actuators for the outerloop acceleration commands. The distribution is done using an externally enforced transition percentage $\varepsilon_\%$ to select the active lifting device, for instance driven by the flightplan or a remote operator. Using this approach the same overall controller architecture can be used to control the UAV in both hovering and forward flight state as well as all states in between and for any given number of lift devices provided that the vehicle aerodynamics allow this.

3.1 Rotors: Thrust-Vectoring Model

In hover, transitioning vehicles like ATMOV are not more than a rotorcraft with a large wing—which in that case acts as a perturbation. Even fixedwing planes can hover using the thrust vectoring model provided they have sufficient thrust and torques. The thrust-vectoring model maps the desired lateral acceleration $\ddot{y}_{cmd}$ di-
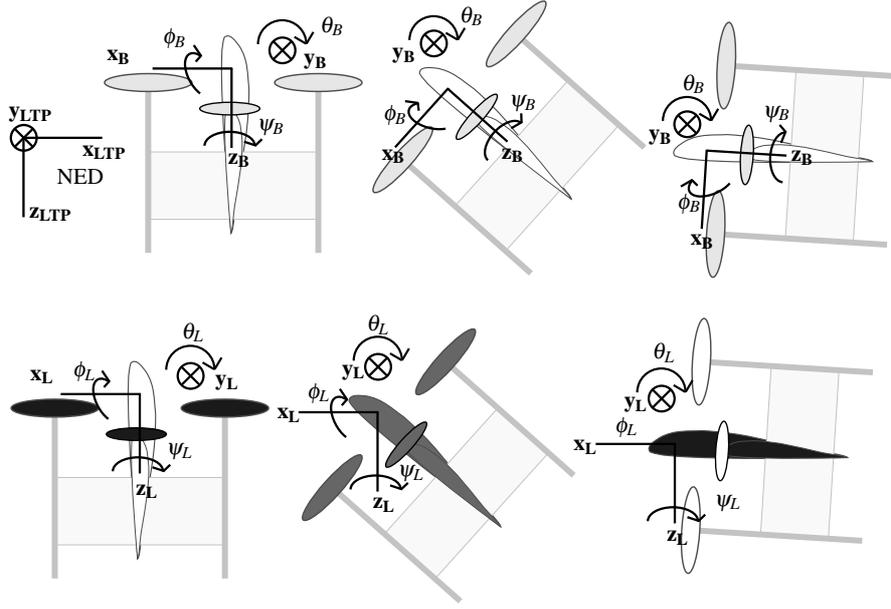
Fig. 3 Axes Definitions ATMOV. Body axes become virtual and can be chosen at any orientation (top). The lift device axes however are always aligned with the z-axis in the opposite direction as the lift and the y pointing right (bottom). The shades of gray indicate the amount to which lifting devices actually contribute to the lift.

rectly to a desired roll angle cmd_ϕ by linearizing $\sin(\phi)\mathbf{g}$ around the hover conditions.

$$cmd_\phi = \arctan\left(\frac{\ddot{y}_{cmd}}{|\mathbf{g}|}\right) \tag{1}$$

$$cmd_\theta = \arctan\left(\frac{\ddot{x}_{cmd}}{|\mathbf{g}|}\right) \tag{2}$$

The terms cmd_ϕ and cmd_θ are with respect to the depicted rotor-lift-axis coordinate system. This mapping from an acceleration command $\ddot{\mathbf{x}}$ to an attitude can also be done in quaternion math, where the norm of the acceleration $|\ddot{\mathbf{x}}|$ is the total thrust and the attitude quaternion is defined by the rotation from the lift-device Z-axis to the lift vector, after applying the heading rotation. In order to do the combination of lift-device commands later we keep the former definition given in Eq. 1.

3.2 Wings: Fixedwing Aircraft Model

In forward flight, even rotorcraft begin to show control couplings that are traditionally classified a fixedwing behavior. Pitch changes for instance become increasingly coupled with the altitude loop as airspeed builds up. To allow forward flight using the same outerloop controller, a fixedwing controller is rewritten to match the rotorcraft inner and outerloop architecture

$$\mathbf{q} = f_{fixed-wing}(\ddot{\mathbf{x}}) \tag{3}$$

This can be achieved by mapping forward acceleration to the throttle, lateral acceleration to roll via the lateral controller and by controlling vertical acceleration with the fixedwing vertical controller that creates elevator and additional throttle commands.

$$cmd_{Thrust} = T_{nominal} + (v_{climb_{set}} - v_{climb}) \ K_{v_z \to T} + (\ddot{x}_{set} - \ddot{x}) \ K_{\ddot{x} \to T} \tag{4}$$

where $T_{nominal}$ is the cruise throttle, $v_{climb_{set}}$ the desired climb speed, $K_{v_z \to T}$ is the so-called `throttle_increment` gain [5] and $K_{\ddot{x} \to T}$ the forward acceleration gain.

$$cmd_\theta = trim_\theta + (v_{climb_{set}} - v_{climb}) \ K_{v_z \to \theta} \tag{5}$$

where $K_{v_z \to \theta}$ is the `pitch_pre_climb` gain in fixedwing control loops in [5]. cmd_ϕ is kept the same for wings as for rotors (Eq. 1), but the heading is forced to follow the coordinated turn equation $m \ \dot{\Psi} \ v = m \ g \ \tan(\phi)$ [16] linearized around the cruise speed v_{cruise}. After isolating $\dot{\Psi}$, assuming constant cruise speed and substituting all constants into one gain K the heading command becomes:

$$cmd_\psi = \int \tan(\phi) \ K_{\dot{\psi}} \tag{6}$$

4 Sustained Transitioned Flight

Whenever the commanded transition percentage $\varepsilon_\%$ is not zero or 100%, several sub-controllers are run in parallel and need to be combined. First a new coordinate system is created with the momentarily active combined lift frame. Then the activations of all lift devices $\kappa_{\%_i}$ is computed to generate the right amount of total lift and finally all sub-control commands are merged.

4.1 Lift Coordinate System

Within each lift device the standard right-hand coordinate system applies, with X pointing to the nose of the lift device and Z pointing opposite to the lift vector (Figs. 3,4). These lift device coordinate systems are called $\mathscr{F}_{Lift_i}$ with i the lift-device index. These lift-device orientation are defined by the rotations q_{Lift_i}. Whenever more than one lift device becomes active, the total lift acts in a new combined lift coordinate system $\mathscr{F}_{Lift}$.

The airframe configuration is then defined as list of n lifting-devices with their relative orientations with respect to the body frame $\mathscr{F}_{Body}$ expressed as quaternions. These quaternions can be seen as a rotation α_{Lift_i} around axis $\mathbf{a}_{Lift_i}$.

$$\mathbf{a}_{Lift_i} = \left[x_{Lift_i}, y_{Lift_i}, z_{Lift_i} \right] \tag{7}$$

$$\beta_i = \frac{\alpha_{Lift_i \to Body}}{2} \tag{8}$$

$$q_{Lift_i \to Body} = \begin{pmatrix} q_i \\ q_x \\ q_y \\ q_z \end{pmatrix}_{Lift_i \to Body} \tag{9}$$

$$q_{Lift_i \to Body} = \begin{pmatrix} \cos \beta_i \\ x_{Lift_i \to Body} \times \sin \beta_i \\ y_{Lift_i \to Body} \times \sin \beta_i \\ z_{Lift_i \to Body} \times \sin \beta_i \end{pmatrix} \tag{10}$$

Obtaining the coordinate system (Fig. 4) in which the transitioned vehicle operates is done by vector manipulations of the unit vector $\mathbf{i}_i$ and $\mathbf{k}_i$ in lift device coordinate systems $\mathscr{F}_{Lift_i}$.
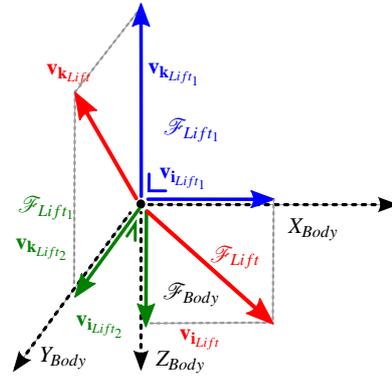
Fig. 4 Lifting device coordinate frames $\mathscr{F}_{Lift_i}$ versus Body frame $\mathscr{F}_{Body}$ and the resulting total transitioned lift frame $\mathscr{F}_{Lift}$.

$$\mathbf{v_{i}}_{Lift_1} = q_{Lift_1 \to Body} \bullet \mathbf{i}_1 \tag{11}$$

$$\mathbf{v_{k}}_{Lift_1} = q_{Lift_1 \to Body} \bullet \mathbf{k}_1 \tag{12}$$

$$\mathbf{v_{i}}_{Lift_2} = q_{Lift_2 \to Body} \bullet \mathbf{i}_2 \tag{13}$$

$$\mathbf{v_{k}}_{Lift_2} = q_{Lift_2 \to Body} \bullet \mathbf{k}_2 \tag{14}$$

These new vectors $\mathbf{v}$ in body reference frame $\mathscr{F}_{Body}$ represent the direction of the lift and nose of each lifting device and can now be scaled depending on the transition percentage $\varepsilon_\%$. The sum of all the scaled active lifting device vectors give the total lift and heading directions

$$\mathbf{v_{i}}_{Lift} = \sum_{i=1}^{n} \left(\mathbf{v_{i}}_{Lift_i} \cdot \varepsilon_{\% i} \right) \tag{15}$$

$$\mathbf{v_{k}}_{Lift} = \sum_{i=1}^{n} \left(\mathbf{v_{k}}_{Lift_i} \cdot \varepsilon_{\% i} \right) \tag{16}$$

$$\tag{17}$$

where n is the amount of lifting devices, i is an index, $\sum$ is a vector sum of the activation-scaled subvectors, $\mathbf{v_{i}}_{Lift}$ is the average heading and $\mathbf{v_{k}}_{Lift}$ the average lift axis. Since the lift devices are most often not inline, the total vectors $\mathbf{v_{i,k}}_{Lift}$ are not necessarily of unit length anymore. The scaling needed to become unity length is called activation percentage and denoted as $\kappa_{\% i}$. These unity scaled orthogonal vectors $\mathbf{v_{i,k}}_{Lift} \cdot \kappa_{\% i}$ now define the reference frame $\mathscr{F}_{Lift}$. In order to find the rotation $q_{Lift \to Body}$, the vectors are written as the columns of a rotation matrix with the cross product as missing column, which then forms a direction cosine matrix that can be converted to a quaternion.

For known configurations like the a dual lifting device vehicle where one lifting device frame corresponds to the body frame, this can be highly simplified to for instance

$$q_{Lift \to Body} = \begin{pmatrix} \cos\left(\frac{\omega_{1 \to 2}}{2}\right) \\ 0 \\ \sin\left(\frac{\omega_{1 \to 2}}{2}\right) \\ 0 \end{pmatrix} \tag{18}$$

where $\omega_{1 \to 2}$ is the magnitude of the angle between the two lift device frames, and we define the rotation is around the body Y axis.

4.2 Lift-Command Merging

So far we have the total lift coordinate system $\mathscr{F}_{Lift}$ given by $q_{Lift \to Body}$ and also the respective activation percentages $\kappa_{\% i}$ for each lift device, both depending on the transition percentage $\varepsilon_\%$. For each device we now define the *lift-device-type*. So

far only thruster and wing types were defined referring to the control loop types
defined in Sect.3.1 and Sect. 3.2 respectively. But more options are possible, like
a lifting device without lateral control, leaving the lateral control entirely to other
lifting devices become possible.

Now each *lift-device-type* has associated control logic in their respective $\mathscr{F}_{Lift_i}$
frames, and the outputs of all outerloop sub-controllers are linearized roll pitch
and yaw commands. Once mapped to the body frame, these commands are linearly
added using the activation percentage $\kappa_{\%_i}$ of that particular lift device.

$$cmd_j = \sum_{i=1}^{n} (cmd_{j_i} \times \kappa_{\%_i}) \tag{19}$$

Where n is the number of lift devices, i the lift device index and j the command
index—respectively a pitch/roll/yaw/thrust commands. A verbal summary of the
difference between both types of lift devices is shown in table 1.

Finally, from this summed command we combine all separate roll, pitch and yaw
commands back to a single attitude quaternion q_{cmd} to be fed to the innerloop.

On the winged quadrotor ATMOV, during flight conditions in between for-
ward flight and hover, both hover commands in the rotor-coordinate system
and fixedwing commands in the fixedwing-coordinate system are calculated.
The total commanded thrust and attitude are averaged according to the lift
device activation depending on the transition percentage $\varepsilon_{\%}$. As both coordi-
nate systems are perpendicular, a 50% activation of both automatically results
in a 45 degree trim attitude with position corrections forward being mapped
to a combined increase in throttle with nose down correction. The throttle
increase comes entirely from the fixedwing controller while the nose down
command comes from the active hover controller. During a climb command
in this transitioned flight, both rotor and wing controllers will increase throttle
and fixedwing will also pitch up a bit, but less than in fully horizontal flight
only.

	Aerodynamic Lift Device	**Thruster Lift Device**
lift (vertical acceleration)	pitch + thrust	thrust
forward acceleration	thrust	pitch
lateral acceleration	roll	roll
heading (bearing?)	two options.	yaw

Table 1 Moment commands sent to the inner loop as result of an acceleration command from the
outer loop to the lift allocation controller

5 Flight-plan Attitude Command

In conventional quadrotor control, flight plans typically only command a position and a heading, since two angles are implied by the thrust vectoring principle. With multiple lifting-device vehicles this principle does not necessarily hold anymore. The *three-pair-of-perpendicular-rotor* hexacopter [7] for instance is capable of hovering at any attitude. In fixedwing airplane mode, on the contrary, when flying coordinated turns all three angles are explicitly defined by the trajectory, requiring no additional attitude commands.

This paper proposes the definition of *active-lift-axis-heading* as missing flight-plan command besides the position. This definition is complete and not over-defined. The *lift-axis-heading* is composed of two aspects: the currently active lift device and a heading around it. The currently active lift device is defined by the transition percentage $\varepsilon_\%$. With 2 lift devices a single variable is needed while additional variables are needed for more lifting devices.

The heading is a more complex definition. Heading is a normally well defined concept, but because of linearization it is often badly used. In North-East-Down axis definitions the heading is defined as the angle with respect to north that the projection of the body x axis makes on the local $x - y$ plane.

On a vehicle that is prone to perform more than 90 degree body axis nose down maneuvers[1], the body heading is not useful anymore in navigation routines. Therefore the current-blended-lifting device axis heading is used instead. To further reduce instabilities in navigation routines when pitch angles get close to 90 degrees, a special definition is used. In the case of 89 degree nose up x-axis, the slightest z-axis rotation causes the Euler defined heading to shift from -90 less to $+90$ more with 90 and -90 degree right roll respectively. This Euler makes the heading angle non-practical as-is. We therefore augmented heading angle to:

$$\psi_{stabilization} = \psi_{LTP \to lift} - \sin(\theta_{LTP \to lift}) \cdot \phi_{LTP \to lift} \tag{20}$$

6 Actuator Staturation with quaternion attitude loops

Actuator saturation suddenly becomes much more important on hybrid—wing-equipped—quadrotors. Compared to traditional quadrotor flight control code, two problems associated with 360 degree quaternion control needed to be solved in order to allow successful flight.

The first is the innerloop quaternion controller. A reference quaternion is given and based on the current attitude quaternion from the AHRS, a shortest rotation quaternion is computed. In the case of highly drifted headings as is quite likely with big wings and wind, this single rotation with a feasible and unfeasible part are not useful anymore. This can be illustrated with a setpoint pointing north with 20

---

[1] In fixedwing descend mode, the body x-axis points to the back of the plane

degrees roll right to accelerate east, while the vehicle has drifted with its nose into the wind and is now pointing east instead of north. The shortest quaternion rotation from the state to the setpoint has a combined 90 degree yaw to the left with 20 degree roll right. Since the yaw part is saturated but the roll is not, only the latter will be executed, resulting in a vehicle banking to the south instead of east. This can be overcome by splitting the control goals into a thrust vector part and a yawing part with different control bandwidths.

The second problem occurs in quadrotor implementations with actuator protection and saturation logic. As in quadrotors the motors are responsible for both lift and torque, safety rules are typically applied to maintain attitude control at extreme total lift. In the paparazzi solution for instance[5], torque commands are deemed more important than the total thrust command. At low throttle, in case of insufficient torque control due to saturation of the slowest rotor, the torque command is maintained by increasing the faster rotor even more, yielding the required torque at the cost of a higher thrust. If this rule is maintained in a hybrid UAV in forward fixedwing flight mode this significant extra thrust on pitch commands is highly undesired.

In case of saturation in the maximum throttle regime however, default quadrotor saturation logic leave only a few percent for pitch control, hereby allowing higher maximum take-off weights on traditional quadrotors. Keeping this rule when a significantly diving ATMOV in fixedwing mode would be put to hover, the low altitude would give full throttle, leaving way too little pitch control for the 135 degree rotation from nose down full throttle flight to hover. This shows that outerloops also need to propagate axis priorities to supervision logic depending on the current flight mode.

7 Implementation and Flight Testing

The ideas proposed in this paper were implemented in the open-source paparazzi project [4]. The used test vehicles were the QuadShot [2] and the ATMOV [1] (Fig 1). Figure 5 shows an excerpt from a manually remotely piloted flight of AT-MOV with several transitions from hover to partial transitionned mode and to full forward flight and back.

The top plot in figure 5 shows the transition percentage ($\varepsilon_{\%}$, black line), the body orentation in lift frame ($\theta_{Lift \Rightarrow Body}$, red line), and the body orientation in LTP frame ($\theta_{Lift \Rightarrow LTP}$ blue line). The center and bottom plot show the position and velocities of the UAV, respectively. At t=440 [s], the pilot sets a 50% transition percentage as plotted in the black line of the top subplot. As the vehicle transitions, a difference grows between the pitch angle θ in LTP and in Lift axes. This is because the active Lift frame turns away from the initially activated rotor axis towards the perpendicularly mounted fixedwing frame. In the ATMOV vehicle the body frame is chosen to be identical to the rotor frame, but the body frame can be chosen freely.
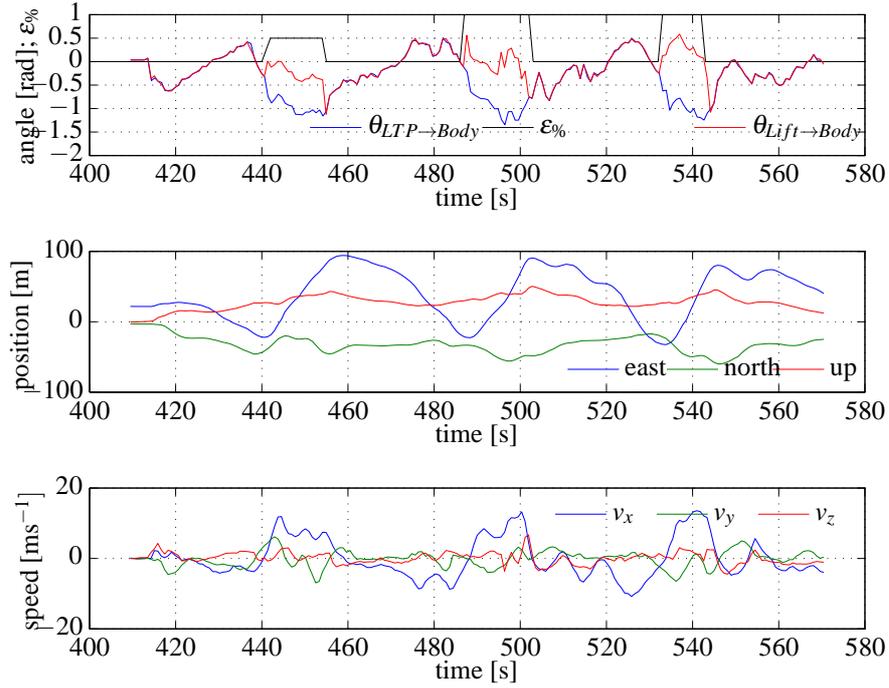
Fig. 5 ATMOV test flight with multiple transitions from hover to forward and back.

During stationary flight the Lift frame on average has its Z-axis parallel to gravity, while the body frame can point in totally different directions. In ATMOV the rotor lifting device and the wing lifting device respectively have a 0 degree and 90 degree rotation around the pitch axis with respect to the body axis. This means the Body X-axis points down in forward flight and even backwards in descending forward flight.

The combination of both lift vectors at 50% activation percentage $\kappa_{\%_i}$ is seen to result a the lift-to-body angle $q_{Lift \rightarrow Body}$ (Eq. 18) which can be interpreted as a body pitch trim angle of 45 degrees nose down, as seen in Fig 5. In other words, the new trim-attitude for the transitioned flight is automatically found from the definitions of the lift-devices and calculated dynamically for every transition percentage $\varepsilon_\%$. In the presented flight log this was selected using a remote control with a 3-position switch selecting either $\varepsilon_\%$, to 0%, 50% or 100%.

The higher horizontal velocity is clearly visible during the moments of forward flight. After hover was restored (at t=460 [s]) by setting the transition percentage to 0%, the vehicle was slowly hovered back to the initial position as depicted in the distance graphs in Fig. 5. In current testflight the transition was selected with a switch, and hense transitions and especially decelerations are quite fast, but the theory allows for slow changes as well since any situation in between is fully stable and controllable. This is illustrated at t=440 [s] with a sustained partial transition.

Besides selecting the transition percentage the remote control was used to steer the position of the ATMOV. During hover phases, the throttle stick was controlling vertical speed and the roll and pitch sticks controlled lateral and forward accelerations while the yaw stick controlled the heading like in normal quadrotor mode. More interestingly however, during the transitions and even during the full forward flight, the throttle stick was still controlling vertical speed, but this time also used the pitch angle to control the vertical speed and used less throttle changes. Similarly the pitch stick was still controlling forward and backward accelerations, but this time did not pitch the vehicle up and down but ended up using throttle of the forward facing propellors to control forward acceleration. This was deduced automatically inflight by the simple but powerful lift-allocation controller.

This approach totally hides the transition percentage of the vehicle from the outerloop and navigation loops yielding identical outerloop and innerloop strategies throughout the hybrid flight.

8 Conclusions

A simple and computationally inexpensive but flexible and powerful approach was discussed to address the control of hybrid or even morphing autonomous vehicles. Using lift-allocation to activate and merge commands from basic controller types like rotors and wings a system is created that allows sustained flight at any transition percentage for any combination of lift-devices. Test flights show seamless transitions while hiding the changed dynamics from the outerloops enabling fully autonomous flights at any transition percentage using the same control structure.

Aspects that need special attention in further work are the propagation of control priorities down to the actuator supervision logic, actuator saturation and more autonomous flights.

References

1. Atmos. URL http://www.teamatmos.com/
2. Quadshot. URL http://www.quadshot.com/
3. Blosch, M., Weiss, S., Scaramuzza, D., Siegwart, R.: Vision based mav navigation in unknown and unstructured environments. In: Robotics and Automation (ICRA), 2010 IEEE International Conference on, pp. 21 –28 (2010). DOI 10.1109/ROBOT.2010.5509920
4. Bouadi, H. and Simoes Cunha, S. and Drouin, A. and Mora-Camino, F.: Adaptive sliding mode control for quadrotor attitude stabilization and altitude tracking. In: Computational Intelligence and Informatics (CINTI), 2011 IEEE 12th International Symposium on, pp. 449 –455 (2011). DOI 10.1109/CINTI.2011.6108547

5. BRISSET, P., A. DROUIN, M. GORRAZ, P.-S. HUARD, J. TYLER: The paparazzi solution. http://www.recherche.enac.fr/paparazzi/papers 2006/mav06 paparazzi.pdf (2006)
6. Croon, G.C.H.E.D., Clercq, K.M.E.D., Ruijsink, R., Remes, B.: Design, aerodynamics, and vision-based control of the DelFly 1(2), 71–98 (2009)
7. D. Langkamp, G. Roberts, A. Scillitoe, I. Lunnon, A. Llopis-Pascual, J. Zamecnik, et co : An engineering development of a novel hexrotor vehicle for 3d applications. In: Proceedings of the International Micro Air Vehicles 2011 Summer Edition (2011). DOI 10.4233/uuid:d7bdec21-938d-426b-9553-59cf834e8061
8. E. Johnson, M. Turbe, A. Wu, S. Kannan, J. Neidhoefer : Flight test results of autonomous fixed-wing uav transitions to and from stationary hover. In: AIAA Guidance, Navigation, and Control Conference and Exhibit. Keystone, Colorado
9. Frank, A.: Hover, Transition, and Level Flight Control Design for a Single-Propeller Indoor Airplane (2007). URL http://citeseerx.ist.psu.edu/viewdoc/summary?doi=10.1.1.93.6304
10. Frank, A., McGrew, J.S., Valenti, M., Levine, D., How, J.P.: Hover, transition, and level flight control design for a single-propeller indoor airplane. In: AIAA Guidance, Navigation, and Control Conference (GNC). Hilton Head, SC (2007 (AIAA 2007-6318)). URL http://acl.mit.edu/papers/GNC_airplane_Aug_2007_v0.pdf
11. Green, W.E., Oh, P.Y.: Autonomous hovering of a fixed-wing micro air vehicle. In: 2006 IEEE INTERNATIONAL CONFERENCE ON ROBOTICS AND AUTOMATION (ICRA), VOLS 1-10, IEEE INTERNATIONAL CONFERENCE ON ROBOTICS AND AUTOMATION, pp. 2164–2169. IEEE, IEEE, 345 E 47TH ST, NEW YORK, NY 10017 USA (2006). IEEE International Conference on Robotics and Automation (ICRA), Orlando, FL, MAY 15-19, 2006
12. Green, W.E., Oh, P.Y.: A hybrid mav for ingress and egress of urban environments. Trans. Rob. 25(2), 253–263 (2009). DOI 10.1109/TRO.2009.2014501. URL http://dx.doi.org/10.1109/TRO.2009.2014501
13. Grzonka, S., Grisetti, G., Burgard, W.: A Fully Autonomous Indoor Quadrotor. Robotics, IEEE Transactions on 28(1), 90–100 (2012). DOI 10.1109/TRO.2011.2162999. URL http://dx.doi.org/10.1109/TRO.2011.2162999
14. Itasse, M., Moschetta, J.M., Ameho, Y., Carr, R.: Equilibrium transition study for a hybrid mav. International Journal of Micro Air Vehicles 3(4), 229–246 (2011)
15. Koichi Kita, Atsushi Konno, and Masaru Uchiyama: Hovering control of a tail-sitter vtol aerial robot. Journal of Robotics and Mechatronics 21(2), 277–283 (2009)
16. Leven, S., Zufferey, J.C., Floreano, D.: A minimalist control strategy for small uavs. In: Intelligent Robots and Systems, 2009. IROS 2009. IEEE/RSJ International Conference on, pp. 2873 –2878 (2009). DOI 10.1109/IROS.2009.5354465
17. Mellinger, D., Michael, N., Kumar, V.: Trajectory generation and control for precise aggressive maneuvers with quadrotors. Int. J. Rob. Res. 31(5), 664–674 (2012). DOI 10.1177/0278364911434236. URL http://dx.doi.org/10.1177/0278364911434236
18. Mellinger, D., Shomin, M., Kumar, V.: Control of quadrotors for robust perching and landing. In: Proceedings of the International Powered Lift Conference (2010)
19. Mellinger, D., Shomin, M., Michael, N., Kumar, V.: Cooperative grasping and transport using multiple quadrotors. In: Proceedings of the International Symposium on Distributed Autonomous Robotic Systems (2010)
20. Michael, N., Mellinger, D., Lindsey, Q., Kumar, V.: The grasp multiple micro uav testbed. IEEE Robotics and Automation Magazine (2010)
21. Naldi, R., Marconi, L.: Optimal transition maneuvers for a class of v/stol aircraft. Automatica 47(5), 870–879 (2011). DOI 10.1016/j.automatica.2011.01.027. URL http://dx.doi.org/10.1016/j.automatica.2011.01.027
22. REUDER, J., B. BRISSET, M. JONASSEN, M. MUELLER, S. MAYER: Sumo: A small unmanned meteorological observer for atmospheric boundary layer research. Earth and Environmental Science 1, doi:10.1088/17551307/1/1/012014 , 10pp. (2008)
23. Stone, H., Clarke, G.: Optimization of transition maneuvers for a tail-sitter unmanned air vehicle (uav). In: Australian Int. Aerospace Congress (p. 105, 2001)